NMR Solution Structure of ImB2, a Protein Conferring Immunity to Antimicrobial Activity of the Type IIa Bacteriocin, Carnobacteriocin B2[†,‡]

Tara Sprules, Karen E. Kawulka, and John C. Vederas*

Department of Chemistry, University of Alberta, Edmonton, Alberta, Canada T6G 2G2

Received June 3, 2004; Revised Manuscript Received July 7, 2004

ABSTRACT: Bacteriocins produced by lactic acid bacteria are potent antimicrobial compounds which are active against closely related bacteria. Producer strains are protected against the effects of their cognate bacteriocins by immunity proteins that are located on the same genetic locus and are coexpressed with the gene encoding the bacteriocin. Several structures are available for class IIa bacteriocins; however, to date, no structures are available for the corresponding immunity proteins. We report here the NMR solution structure of the 111-amino acid immunity protein for carnobacteriocin B2 (ImB2). ImB2 folds into a globular domain in aqueous solution which contains an antiparallel four-helix bundle. Extensive packing by hydrophobic side chains in adjacent helices forms the core of the protein. The C-terminus, containing a fifth helix and an extended strand, is held against the four-helix bundle by hydrophobic interactions with helices 3 and 4. Most of the charged and polar residues in the protein face the solvent. Helix 3 is well-defined to residue 55, and a stretch of nascent helix followed by an unstructured loop joins it to helix 4. No interaction is observed between ImB2 and either carnobacteriocin B2 (CbnB2) or its precursor. Protection from the action of CbnB2 is only observed when ImB2 is expressed within the cell. The loop between helices 3 and 4, and a hydrophobic pocket which it partially masks, may be important for interaction with membrane receptors responsible for sensitivity to class IIa bacteriocins.

Bacteriocins produced by lactic acid bacteria (LAB)[1] are ribosomally synthesized antimicrobial peptides that are active against related Gram-positive bacteria but generally display no toxicity toward humans or other eukaryotes (*1*−*3*). Although some are lantibiotics (*1*, *4*−*6*) that undergo very extensive post-translational modifications, such as formation of dehydro residues and lanthionine bridges, a significant number are only processed by cleavage of a leader peptide during cellular export of the mature bacteriocin. Among the latter group, the class IIa bacteriocins ("pediocin-like bacteriocins") are single peptides characterized by a conserved YGNGVXC motif in the N-terminus, with the cysteine involved in a disulfide bridge (*3*, *7*−*9*). In 1991, we reported the purification and the primary structure of the first of this class, leucocin A (leuA) (*10*), but now more than 20 such peptides have been identified, with carnobacteriocin B2 (CbnB2) (*11*) being the largest thus far (Figure 1). These heat stable, cationic peptides typically have 37−48 amino acid residues and display potent activity against the food pathogen *Listeria monocytogenes*. Such bacteriocins and the LAB that produce them are effective nontoxic food preservatives and have exciting potential applications in human and veterinary medicine.

The solution structures of three class IIa bacteriocins (leuA, CbnB2, and sakacin P) have been reported (*34*−*36*), as has the structure of the unprocessed precursor peptide, precarnobacteriocin B2 (*37*). These results, in conjunction with recent temperature-dependent circular dichroism and molecular dynamics studies (*38*) as well as numerous reports on structure−activity relationships (*7*, *39*−*41*), suggest that the amphipathic α-helix near the C-terminus is critical for antimicrobial activity. This is the region of the bacteriocins with a lower degree of sequence homology, both between and within each of the three groups (Figure 1). The mechanism is likely to involve recognition of a membrane-bound receptor protein in sensitive target cells (*39*). The target receptor for class IIa bacteriocins appears to include one or more proteins of the mannose phosphotransferase system, namely, EII_t^{man} (*42*−*45*).

The structural genes for class IIa bacteriocins are usually near and coexpressed with a gene for an immunity protein, typically encoding 88−115 amino acids, that protects the organism from the antimicrobial action of its bacteriocin (Figure 2). The immunity proteins are usually quite specific for a particular bacteriocin (*13*). The amino acid sequences of most immunity proteins of class IIa bacteriocins have been reported, and have recently been classified into three groups based on sequence homology (*13*). In contrast to the bacteriocins, the degree of homology between the immunity proteins is more varied. The immunity proteins in group B

[†] These investigations were supported by the Natural Sciences and Engineering Council of Canada (NSERC), the Alberta Heritage Fund for Medical Research (AHFMR), and the Canada Research Chair in Bioorganic and Medicinal Chemistry.

[‡] Atomic coordinates for ImB2 have been deposited in the Protein Data Bank as entry 1TDP. Chemical shifts have been deposited in the BioMagRes Bank as entry 6211.

* To whom correspondence should be addressed. Telephone: (780) 492-5475. Fax: (780) 492-8231. E-mail: john.vederas@ualberta.ca.

[1] Abbreviations: LAB, lactic acid bacteria; LeuA, leucocin A; CbnB2, carnobacteriocin B2; ImB2, carnobacteriocin B2 immunity protein; MBP, maltose binding protein; HSQC, heteronuclear single-quantum coherence; preCbnB2, precarnobacteriocin B2; NOE, nuclear Overhauser effect.

10.1021/bi048854+ CCC: $27.50
Published on Web 08/26/2004

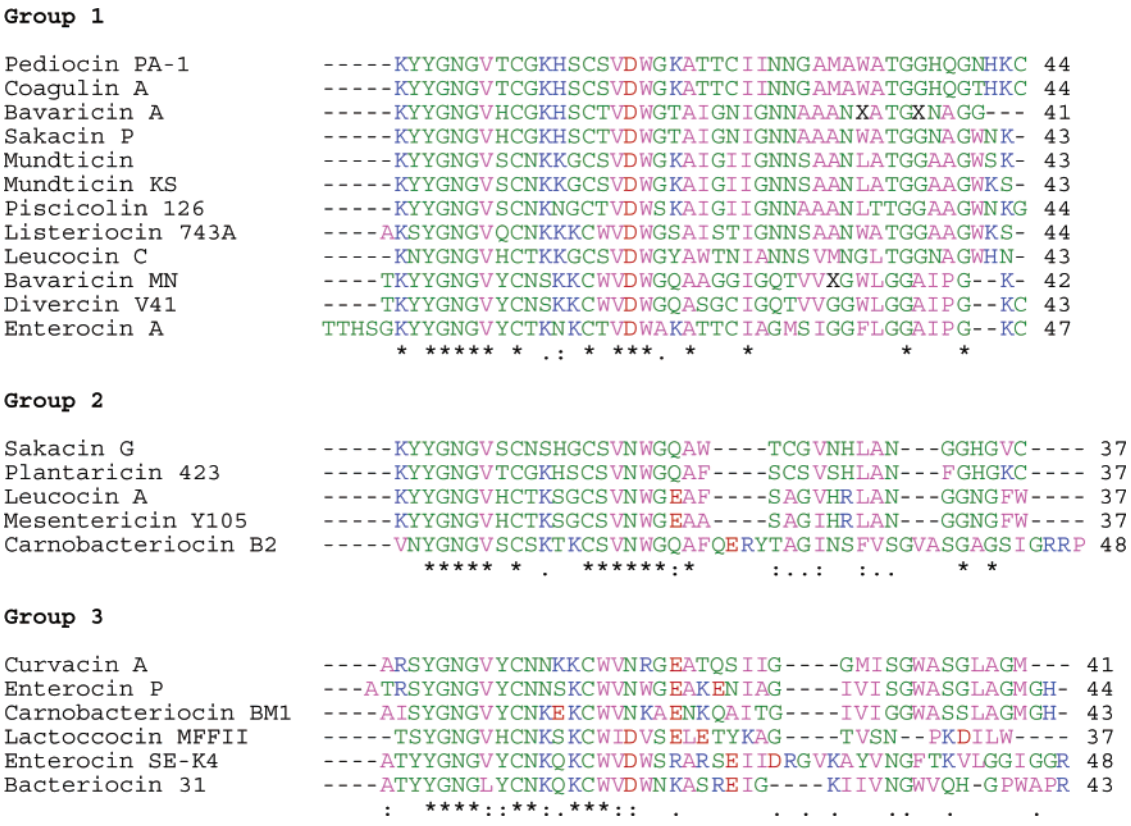

FIGURE 1: Sequence alignment of class IIa bacteriocins. Class IIa bacteriocin sequences were aligned using ClustalW (*12*) and arranged into groups based on similarities in the C-terminal region as in Fimland et al. (*13*): group 1, pediocin PA-1 (*14*), coagulin (*15*), bavaricin A (*16*), sakacin P (*17*), mundticin (*18*), mundticin KS (*19*), piscicolin 126 (*20*), listeriocin 743A (*21*), leucocin C (*22*), bavaricin MN (*23*), divercin V41 (*24*), and enterocin A (*25*); group 2, sakacin G (*26*), plantaricin 423 (*27*), leucocin A (*10*), mesentericin Y105 (*28*), and carnobacteriocin B2 (*11*); and group 3, curvacin A (*29*), enterocin P (*30*), carnobacteriocin BM1 (*11*), lactococcin MFFII (*31*), enterocin SE-K4 (*32*), and bacteriocin 31 (*33*). Amino acids are colored according to physicochemical characteristics as follows: blue for basic, red for acidic, magenta for hydrophobic, and green for polar (and glycine). Conserved residues within each group are denoted with an asterisk, conservative substitutions with a colon, and semiconservative substitutions with a period.

contain a large number of identical and conservatively substituted residues. The corresponding bacteriocins are also very similar to one another. Less homology is observed in groups A and C, with a higher level of conservation in the C-terminal portions of the proteins (see below). The immunity protein ImB2 (111 amino acid residues), which confers resistance to CbnB2, is somewhat unusual in that its length is similar to the lengths of immunity proteins in group A, but its sequence is the most homologous to that of group C (Figure 2). The mode of action of these immunity proteins is not known. Early studies on the immunity proteins for CbnB2 (i.e., ImB2) (*11*) and mesentericin Y105 (*48*) suggest that they act within the cell to confer resistance to extracellular bacteriocin. Addition of purified ImB2 to media containing a sensitive organism offered no protection against the bacteriocin, but expression of its structural gene within the cells made them fully resistant (*49*). A very recent report on hybrid immunity proteins indicates that the C-terminal half contains a domain that is involved in specificity of recognition of a particular bacteriocin (*50*). Moreover, the results show that the effectiveness of such immunity proteins is dependent on the strain wherein they are expressed. This suggests that the immunity proteins of class IIa bacteriocins recognize and bind to target protein(s) produced by the particular organism. In this study, we describe the aqueous solution structure of ImB2, the immunity protein which protects against the action of CbnB2, using isotopic labeling and NMR analysis. This is the first three-dimensional structure of an immunity protein for a class IIa bacteriocin. The results show that ImB2 is well-structured in water as a four-helix bundle with a fifth helix arranged perpendicularly across helix 3. A flexible loop in the C-terminal portion encompassing residues 58−74 may be involved in recognition of a target protein, possibly in the mannose phosphotransferase system EII_t^{man}, which could thereby block the action of the bacteriocin CbnB2 without directly binding to it.

MATERIALS AND METHODS

Purification of ImB2. *Escherichia coli* BL21(DE3) cells transformed with the plasmid pLQ300i (*49*), expressing ImB2 as a maltose binding protein (MBP) fusion, were grown with shaking at 37 °C in M9 minimal medium containing 100 μg/mL ampicillin with $(^{15}NH_4)_2SO_4$ and [U-^{13}C]-D-glucose (99% isotopic purity, Cambridge Isotope Laboratories, Woburn, MA) as the sole nitrogen and carbon sources, respectively. Recombinant protein production was induced with 0.3 mM isopropyl 1-thio-β-D-galactopyranoside when the optical density at 600 nm of the cell culture reached 0.5. The culture was incubated for a further 3 h at 37 °C, and the cells were harvested by centrifugation. The cell pellet was resuspended in column buffer [20 mM Tris-HCl (pH 7.6), 200 mM NaCl, 1 mM EDTA, 1 mM NaN_3, and 1 mM DTT; 40 mL/liter of cell culture]; lysozyme (0.1 mg/mL)

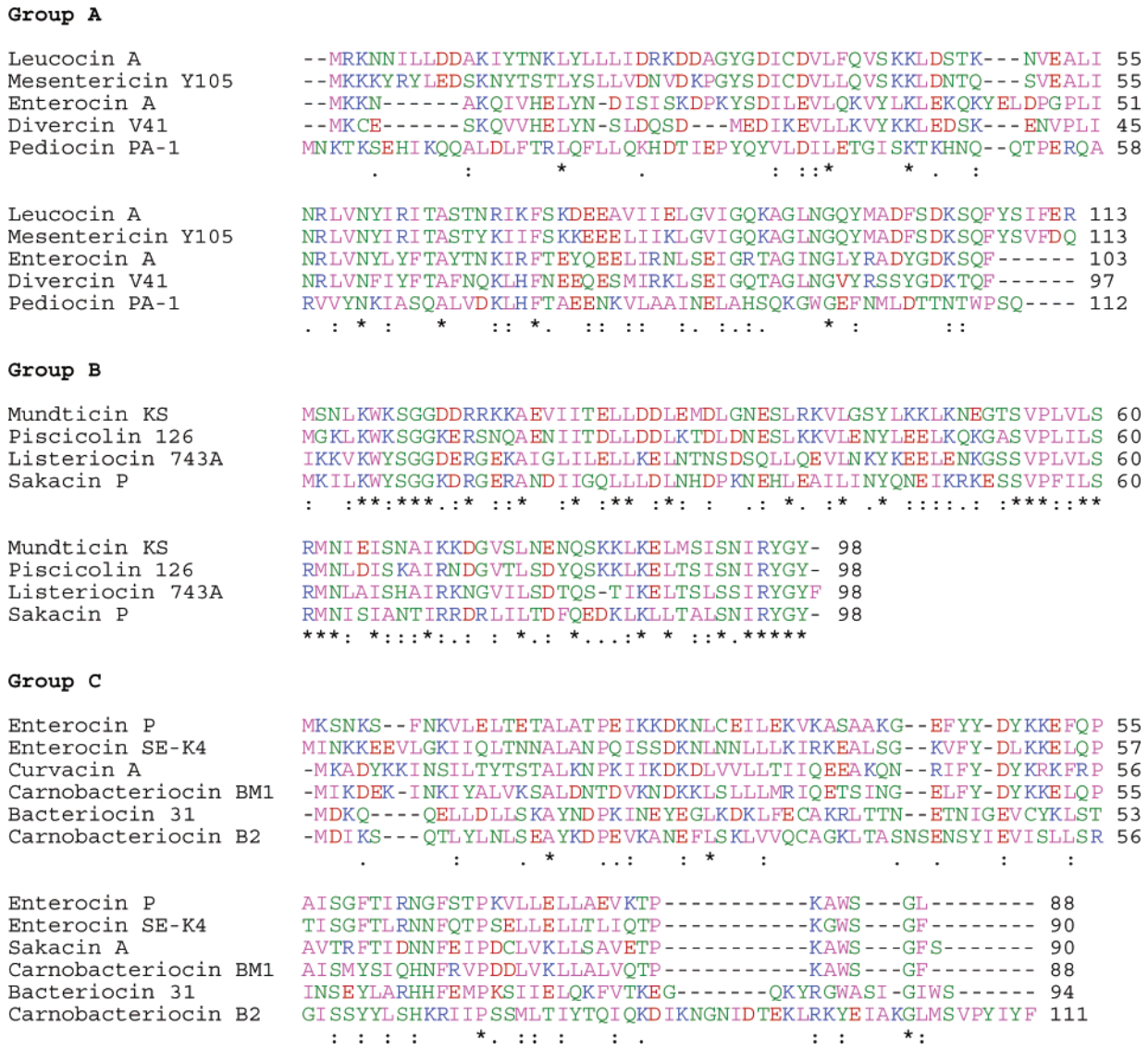

FIGURE 2: Sequence alignment of (putative) immunity proteins for class IIa bacteriocins. The sequences for immunity proteins corresponding to class IIa bacteriocins were aligned using ClustalW (*12*) and arranged into groups according to sequence alignment and phylogenetic analysis as in Fimland et al. (*13*): group A, leucocin A (*10*), mesentericin Y105 (*28*), enterocin A (*46*), divercin V41 (*24*), and pediocin PA-1 (*14*); group B, mundticin KS (*19*), piscicolin 126 (*20*), listeriocin 743A (*21*), and sakacin P (*17*); and group C, enterocin P (*30*), enterocin SE-K4 (*32*), curvacin A (*47*), carnobacteriocin BM1 (*11*), bacteriocin 31 (*33*), and carnobacteriocin B2 (*11*). Amino acids are colored according to physicochemical characteristics as follows: blue for basic, red for acidic, magenta for hydrophobic, and green for polar (and glycine). Conserved residues within each group are denoted with an asterisk, conservative substitutions with a colon, and semiconservative substitutions with a period.

was added, and the suspension was frozen at −70 °C overnight. The resuspended cell pellet was then thawed and lysed by sonication. The cells were centrifuged, applied to a column of amylose resin (New England Biolabs), washed with column buffer, and eluted with 10 mM maltose, according to the manufacturer's protocol. The resulting protein solution was dialyzed against factor Xa cleavage buffer [20 mM Tris-HCl (pH 8.0), 100 mM NaCl, and 2 mM $CaCl_2$]. ImB2 was cleaved from MBP with factor Xa (10 μg/mg) (Protein Engineering Technology, Aarhus, Denmark) overnight at room temperature. The sample was then passed over Q-Sepharose (Pharmacia) to remove factor Xa and MBP. ImB2 was dialyzed against a solution of 20 mM sodium phosphate (pH 6.6), 25 mM NaCl, 1 mM DTT, and 1 mM EDTA. The protein was concentrated in Amicon Ultra centrifugal concentrators (Millipore), spun at 3700*g*. Spin times were limited to 10 min, at which point the solution being concentrated was gently mixed before further centrifugation to avoid precipitation of the protein. ImB2 was concentrated to 0.8 mM and transferred to susceptibility-matched Shigemi NMR tubes. A sample of [^{13}C,^{15}N]ImB2 in a ca. 98% D_2O/2% H_2O mixture was prepared by repeatedly concentrating a sample prepared as described above and diluting it with buffer containing 100% D_2O.

NMR Spectroscopy. Most NMR experiments were carried out on a Varian INOVA-600 spectrometer. A series of ^{15}N HSQC spectra were recorded at 11, 15, 20, 25, 28, and 35 °C. The most appropriate temperature for further experiments was determined to be 15 °C, as amide cross-peaks for residues 55−74 became broader and began to disappear as the temperature was increased. Small improvements in spectral dispersion were also observed at lower temperatures. Below 15 °C, the differences in the spectra were not significant. ^{15}N HSQC-TOCSY (60 ms spin lock) (*51*, *52*),

^{15}N HSQC-NOESY (50 and 150 ms mixing times) (*51*, *52*), and HNHA (*53*, *54*) experiments were carried out for a sample of ^{15}N-labeled ImB2. HNCO, HNCA (*55*−*58*), HNCACB (*57*−*59*), and CBCA(CO)NH (*60*) spectra were recorded for a sample of ^{13}C- and ^{15}N-labeled ImB2 in a 90/10 H_2O/D_2O mixture. The ^{13}C HSQC, ^{13}C HCCH-TOCSY (*61*), and ^{13}C HSQC-NOESY (*62*) spectra were recorded for a sample of ImB2 in deuterated solvent on the Varian INOVA-800 spectrometer at the National High Field Nuclear Magnetic Resonance Centre (NANUC, Edmonton, AB). Chemical shifts were referenced to an internal standard of DSS (*63*). Data were processed with NMRpipe (*64*), and data analysis was performed with NMRView (*65*). Data were multiplied by a 90°-shifted sine-bell squared function in all dimensions. Indirect dimensions were doubled by linear prediction and zero-filled to the nearest power of 2 prior to Fourier transformation.

Titration of ImB2 with PreCbnB2 and CbnB2. PreCbnB2 and CbnB2 were prepared as described previously (*40*) and dissolved in the same buffer as ImB2. ^{15}N HSQC spectra of ImB2 were recorded in the presence of 0.25, 0.5, and 1 equiv of preCbnB2 and 0.3 and 1.5 equiv of CbnB2. No changes in the spectrum of ImB2 were observed.

Structure Calculations. A total of 2118 NOE restraints were obtained from ^{15}N- and ^{13}C-edited HSQC-NOESY experiments, and classified as strong, medium, and weak, corresponding to distance restraints of 1.8−3.0, 1.8−4.0, and 1.8−5.0 Å, respectively. Sixty backbone ϕ angles were obtained from analysis of the diagonal-peak to cross-peak intensity ratio in the HNHA experiment with torsion angles calculated from the Karplus equation (*53*) and assigned an error of ±15°. Seventy backbone ψ angle restraints were obtained from analysis of $d_{N\alpha}/d_{\alpha N}$ ratios (*66*). The ψ angle restraint was set to $-30 \pm 110°$ for $d_{N\alpha}/d_{\alpha N}$ ratios of <1 and to $120 \pm 100°$ for $d_{N\alpha}/d_{\alpha N}$ ratios of >1. Amide protons whose temperature coefficient was more positive than −3.5 ppb/K, and which were located within an α-helix (based on NOE and chemical shift data), were assumed to be hydrogen-bonded (*67*). Initially, 100 structures were calculated with CNS version 1.1 (*68*), using torsion angle dynamics and the default parameters in the anneal.inp input file. A total of 732 intraresidue, 534 sequential, 566 medium-range, and 286 long-range NOEs were employed in the first round of structure calculations. The resulting structures were subjected to a second round of simulated annealing with the addition of 84 hydrogen bond restraints and 130 dihedral angle restraints, determined as described above. The 15 lowest-energy accepted structures (no NOE violations of >0.5 Å, no dihedral angle violations of >5°) with no residues in the disallowed region of the Ramachandran plot (excluding the loop of residues 58−72) were chosen to represent the structure of ImB2.

RESULTS AND DISCUSSION

Chemical Shift Assignment. ImB2 is a 111-amino acid protein containing 12 leucines, 12 isoleucines, 11 lysines, and 14 serines (44% of the molecule). To assist NMR assignment, samples of [^{15}N]ImB2 and [^{13}C,^{15}N]ImB2 were generated by fermentation in appropriately labeled medium of *E. coli* BL21(DE3) cells transformed with the plasmid pLQ300i, expressing ImB2 as a maltose binding protein (MBP) fusion (*49*). Purification of the fusion protein and subsequent cleavage with factor Xa afforded the corresponding labeled immunity proteins having >98% ^{13}C and ^{15}N. Despite the multiplicity of similar residues, the cross-peaks in the ^{15}N HSQC spectrum are well-dispersed, with very little overlap for 101 of 108 expected amide protons that can be assigned (Figure 3). Sequential chemical shift assignments for ImB2 were obtained by analysis of HNCA, CBCA(CO)NH, and HNCACB experiments. Nearly complete backbone and side chain ^{1}H, ^{15}N, and ^{13}C assignments were obtained (96%, with 99 residues of 111 fully assigned). The residues for which complete assignments were not obtained fall in the region between amino acids 55 and 74. Amide cross-peaks were broad and weak for residues 56,

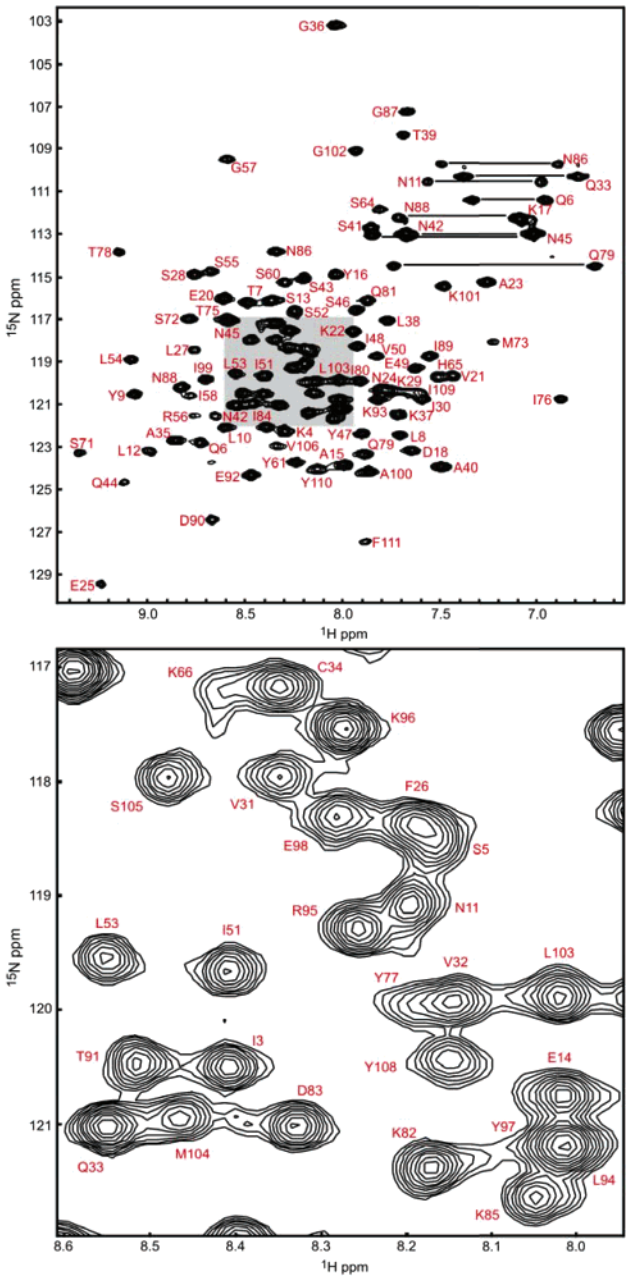

FIGURE 3: ^{15}N HSQC spectrum of ImB2. The 600 MHz spectrum was recorded on 0.8 mM ImB2 in 20 mM sodium phosphate (pH 6.6) and 25 mM NaCl at 15 °C. Amide cross-peaks and Asn and Gln side chains are labeled with the corresponding residue. The central portion (shaded) of the top spectrum is enlarged in the bottom panel for clarity.

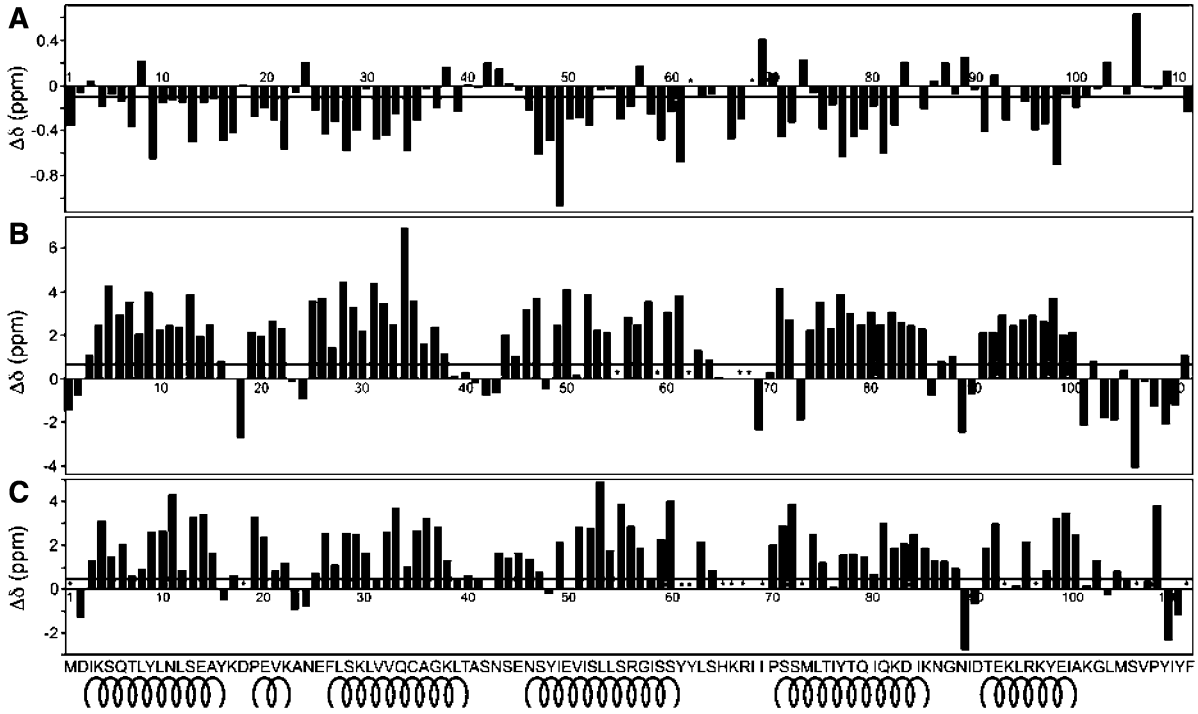

FIGURE 4: Secondary chemical shifts: (A) ^{1}Hα chemical shifts, (B) ^{13}Cα chemical shifts, and (C) ^{13}CO chemical shifts. The difference between the observed chemical shift and the random coil value is plotted against residue number (*69*). Atoms for which a chemical shift could not be determined are denoted with asterisks. A bold line indicates the cutoff below which (^{1}Hα) or above which (^{13}Cα and ^{13}CO) the secondary chemical shift is indicative of α-helical character. The amino acid sequence and cartoons indicating the positions of the α-helices in ImB2 are shown at the bottom.

58, 65, 66, 69, and 73 and either overlapped or missing for residues 62, 63, 67, 68, and 74 in ^{15}N HSQC spectra. Some of the side chain ^{1}H−^{13}C cross-peaks for these residues were also not observed in ^{13}C HSQC spectra. Side chain assignments for residues 55, 59, 62, 67, 68, and 71 were partially determined. Higher temperature (28 °C vs 15 °C) resulted in further broadening of the amide cross-peaks in this region and allowed even fewer assignments to be made. Only intraresidue or $i + 1$ NOEs were observed for 10 of the 20 amino acid residues in this small section of the protein, which is relatively unstructured and forms a conformationally flexible section (see below). Secondary chemical shift analysis for the α, *β*, and carbonyl carbons that were assigned up to residue 64 is indicative of α-helical structure (*69*) (Figure 4). Because of a lack of NOE data, helix 3 is well-defined until only S55 (see below). The nascent helical structure in this region may be forming and dissociating on the NMR time scale, resulting in averaging of chemical shifts and broad peaks that cannot be observed.

Structure of Carnobacteriocin B2 Immunity Protein. The structure of ImB2 was calculated on the basis of 2118 NOEs, 130 dihedral angles, and 84 hydrogen bonds. ImB2 consists of five α-helices, a short turn of α-helix between helices 1 and 2, an unstructured/nascent helix region, and an extended C-terminus (Figure 5). Helices 1−4 form an antiparallel four-helix bundle, folding around a well-defined hydrophobic core. Each helix is 14 or 15 amino acids long. Helix 3 is kinked in the middle. The C-terminal half packs in the helical bundle, and the N-terminal half interacts with helix 5. The hydrophobic side chains of the four-helix bundle pack tightly in the interior on the basis of the observation of numerous interhelix NOEs (Figure 6). α-Helices preferentially pack together with interhelical angles of 20° and 50°, and the

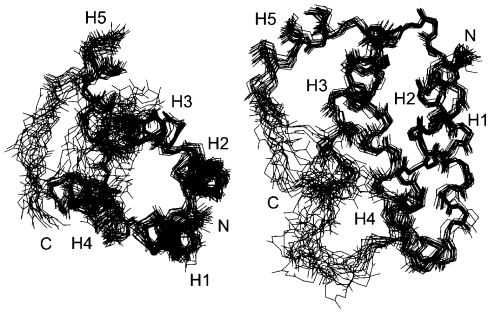

FIGURE 5: NMR solution structure of ImB2. Superposition of 15 structures on the backbone of the α-helices. The positions of the N- and C-termini and the five α-helices are given. On the left is a view down the axis of the four-helix bundle, which is rotated 90° in the plane of the page so that the structures can be viewed from the side in the right panel.

"ridges-into-grooves" model describes intercalations of ridges and grooves formed by residues three positions apart ($i - 3$, i, $i + 3$, ...) and four positions apart ($i - 4$, i, $i + 4$, ...) in sequence (*70*, *71*). Angles of 23°, 15°, 28°, and 11° are found between the pairs formed by helices 1 and 2, helices 2 and 3, helices 3 and 4, and helices 1 and 4, respectively. Intercalation of $i + 4$ residues S5, F9, and S13 in helix 1 and $i + 3$ residues L38, A35, and V32 in helix 2 is observed, as are the corresponding $i + 3$−$i + 4$ interactions of F9, L12, and A15 with T39, A35, and V31, respectively. Similar interactions are observed between the other α-helical pairs. As expected, the polar side chains face the aqueous exterior. No long-range NOEs are observed for T7, S10, or E14 in helix 1, E25, K29, Q33, G36, or K37 in helix 2, and T78, Q81, K82, or K85 in helix 4. Helix 5 and the C-terminus pack in a roughly perpendicular fashion across helices 3 and 4. The fifth helix is held across the four-helix bundle by

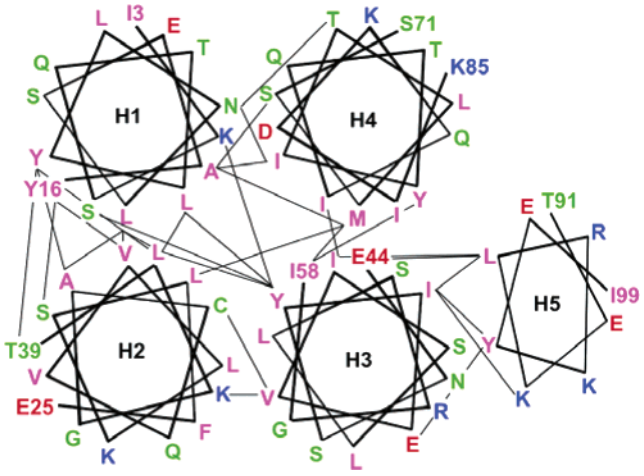

FIGURE 6: Helical wheel representation of ImB2. Helical wheels are shown for the five α-helices in ImB2. Amino acids are colored according to residue type: blue for basic, red for acidic, magenta for hydrophobic, and green for polar. Long-range NOEs between amino acid residues that form the hydrophobic core of the protein are denoted with thin lines. H5 is distorted to illustrate that it is perpendicular to the four-helix bundle.

Table 1: Structure Statistics for ImB2

total no. of NOE restraints	2118
intraresidue	732
sequential ($\|i-j\|=1$)	534
medium-range ($1<\|i-j\|\leq 4$)	566
long-range ($\|i-j\|>4$)	286
no. of hydrogen bonds	84
no. of dihedral angle restraints	130
statistics for structure calculation	**$\langle\overline{SA}\rangle$[a]**
rmsd from idealized covalent geometry	
bonds (Å)	0.0056 ± 0.0002
bond angles (deg)	0.66 ± 0.02
improper torsions (deg)	0.58 ± 0.02
rmsd from experimental distances (Å)[b]	0.040 ± .002
final energies (kcal/mol)	
E_{total}	850 ± 55
E_{bonds}	57 ± 5
$E_{impropers}$	46 ± 4
E_{vdW}[c]	256 ± 17
E_{NOE}	260 ± 22
coordinate precision[d] (Å)	**$\langle\overline{SA}\rangle$ vs $\langle SA\rangle$**
rmsd of all backbone atoms (N, Cα, C′)	1.69 ± 0.30
rmsd of all heavy atoms	2.64 ± 0.37
rmsd of all backbone atoms, residues 3−55 and 75−99	0.76 ± 0.13
rmsd of all heavy atoms, residues 3−55 and 75−99	1.35 ± 0.14

[a] $\langle\overline{SA}\rangle$ refers to the ensemble of 15 structures. [b] No NOEs were violated by more than 0.40 Å. [c] Scale factor for the final van der Waals (repel) energy term = 1.0. [d] The rmsd between the ensemble of structures $\langle\overline{SA}\rangle$ and the average structure of the ensemble $\langle SA\rangle$.

hydrophobic interactions of the side chains of residues K93, L94, and Y97 with residues Q44, Y47, I48, and I51 in helix 3. Corresponding interactions of residues Y108, I109, and Y111 with residues L74 and Y77 in helix 4 help hold the C-terminal region in place. The overall rmsd for the backbone atoms of the entire protein is 1.7 Å. When only the well-defined helical regions are taken into account, it is 0.76 Å (Table 1). As mentioned above, helix 3 is well-defined to residue S55, and NOEs indicative of helical structure are observed to residue I58. From residues 58−71, a relatively

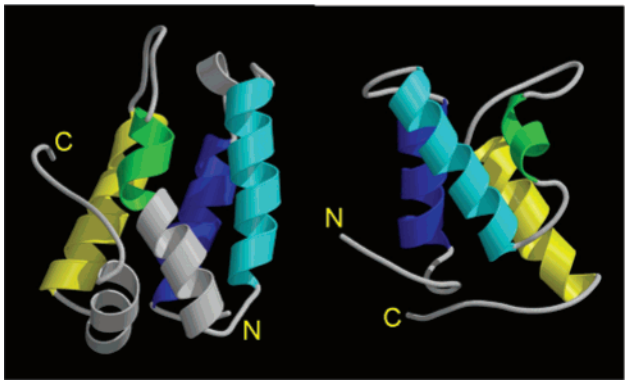

FIGURE 7: Comparison of the structures of the carnobacteriocin B2 immunity protein (ImB2) and the colicin E9 immunity protein (ImmE9) (PDB entry 1IMQ). The helices forming the four-helix bundle are colored the same in each structure: helix 1 in blue, helix 2 in cyan, helix 3 in green, and helix 4 in yellow. Colicin E9 binds to helices 2 and 3 (cyan and green, respectively) of ImmE9, with additional interactions in the loop connecting helices 3 and 4.

unstructured loop is apparent. Data indicate a nascent helix structure can be present up to residue 64. This region may be important for binding a putative receptor in the cell membrane (see below).

Comparison to Colicin Immunity Proteins. To date, the only bacteriocin immunity proteins whose three-dimensional structures have been solved are those for the unrelated colicins of the Gram-negative organism *E. coli*. Immunity protein and immunity protein−colicin complex structures have been reported for colicins E3 and E7−E9, all of which are DNases or RNases (*72*−*79*). Despite the difference in activity between these hydrolytically active colicin enzymes and the class IIa bacteriocins of Gram-positive LAB, there are some common structural features between the colicin immunity proteins (for E7−E9) and the ImB2 immunity protein (Figure 7). Both are four-helix bundles, consisting of antiparallel helices folding around a hydrophobic core. The ImB2 immunity protein is a left-turning bundle, whereas the colicin immunity proteins are right-turning. Helices 1, 2, and 4 are similar in length, ranging from 12 to 16 amino acids each. Helix 3 of the colicin immunity proteins is atypically short in comparison to most four-helix bundles. While helix 3 of ImB2 is similar to the other three helices in length, closer inspection reveals that a kink discriminates between the N-terminal half, which packs against helix 5, and the shorter C-terminal portion (colored green in Figure 7), which forms part of the four-helix bundle. These *E. coli* immunity proteins (87 amino acids) are shorter than most class IIa immunity proteins (typically 88−113 amino acids) (*13*). The colicin immunity proteins do not bind directly in the cleft where the nucleic acid binds, but rather, their binding position interferes with the ability of the nucleic acid to fit in its cleft completely (*78*, *80*, *81*). Conserved hydrophobic residues form a large part of the binding interface, but mutational studies have shown that variable residues determine the specificity of the interaction. In the case of the pore-forming colicins, whose activity is much more similar to those of class IIa bacteriocins, no structures are available for the immunity proteins, although it is known that they are transmembrane proteins residing in the cytoplasmic membrane, and bind the C-terminal channel domain of their colicins, resulting in blockage of pores (*82*, *83*).

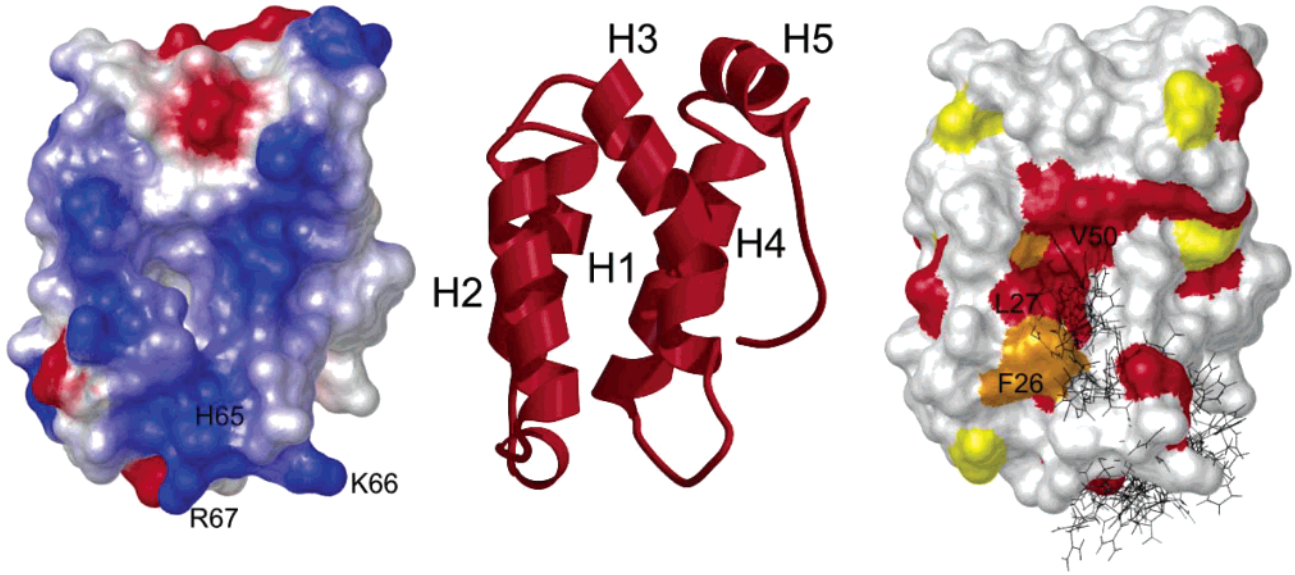

FIGURE 8: Surface representations of ImB2. At the left is a surface representation of ImB2 colored according to electrostatic potential (blue for positive and red for negative). The basic residues in the flexible loop are labeled, and the hydrophobic pocket formed by the H2 and H3 helices can be see in the center flanked by the blue surfaces. In the center is a ribbon representation of ImB2 in the same orientation for reference. At the right is a surface representation of ImB2 with residues colored according to hydrophobicity (red for Ile, Leu, and Val, orange for Phe and Cys, and yellow for Ala and Met). The side chains of residues 61−69 (loop) for the ensemble of structures are also illustrated to indicate their partial overlay of the hydrophobic pocket. Figures were generated with Molmol (*85*, *89*) and Molscript (*86*).

Lack of Interaction of Immunity Protein ImB2 with Its Bacteriocin CbnB2 and a Possible Mechanism of Action. The mechanism by which class IIa bacteriocin immunity proteins work to prevent attack by their innate bacteriocins is not yet understood. No significant interaction between ImB2 and CbnB2 could be observed in earlier studies using microtiter plate assays (*49*). As mentioned above, extracellular addition of immunity protein affords no protection against the action of the cognate class IIa bacteriocin, but expression within cells renders them completely immune to external addition of bacteriocin to cultures (*13*, *49*, *50*, *84*). In the work presented here, we used NMR analysis to reconfirm the absence of direct interaction between ImB2 and its bacteriocin CbnB2. A 0.4 mM sample of [^{15}N]ImB2 immunity protein was titrated with 1.5 molar equiv of CbnB2. No change in the ^{15}N HSQC of the ImB2 was observed. Analogous experiments with the bacteriocin precursor, PreCbnB2, also did not show any effect on the ^{15}N HSQC of labeled ImB2. Although ImB2 displays well-defined structure in water, both CbnB2 and CbnB2P are unstructured in water and assume a defined conformation in only trifluoroethanol or membrane-mimicking environments, such as dodecylphosphocholine micelles (*35*, *37*). The lack of interactions in these assays, in conjunction with other studies (*13*, *49*, *50*, *84*), clearly demonstrates that the immunity protein does not work by sequestering the bacteriocin while it is in the cytoplasm, either as the precursor or as the mature peptide. These data do not strictly preclude direct interaction at the cell membrane, which could possibly occur if conformational changes transpire in either or both of the partners as a consequence of lipid binding. However, this appears to be unlikely on the basis of the inability of externally administered ImB2 to protect against CbnB2 (*49*) and the variations of immunity protein effectiveness depending on the organism in which they are expressed (*13*). In addition, recent circular dichroism studies indicate that little if any change occurs in conformations of immunity proteins for class IIa bacteriocins upon switching solvents from water to dodecylphosphocholine micelles or dioleyl-L-α-phosphatidylglycerol liposomes (*50*).

Several regions of ImB2, which is found in the cytoplasm (*49*), may be important for its function and possible protein−protein interactions. No transmembrane helices are predicted in ImB2, and the structure demonstrates that most hydrophobic residues are in the center of a four-helix bundle and the exterior displays more charged and hydrophilic residues. A large stretch of nascent α-helix, followed by a loop, is found between residues 58 and 72. At the end of the nascent helix is a stretch of three basic residues, namely, H65, K66, and R67 (Figure 8). As these are positively charged in the producing cell, they could play a role in attracting or binding ImB2 to the cell membrane. ImB2 may then interact with a membrane-bound receptor protein to prevent pore formation and/or cell lysis. This variable region also partially overlays a hydrophobic pocket formed by residues F26, L27, L30, and V31 in the N-terminus of helix 2 and L54, L53, and V50 of helix 3 (Figure 8), which could be very important for protein−protein interactions in proposed receptor recognition and binding. Hydrophobic residues are found at positions corresponding to ImB2 residues 27, 30, 31, 50, and 54 in both group A and group C immunity proteins (Figure 2). Conserved hydrophobic residues in helix 3 of the colicin immunity proteins also mediate protein−protein interactions, with nonconserved residues in helix 2 providing specificity of binding (*78*). The mechanism of ImB2 may be similar to that proposed for the immunity protein that protects against the LAB bacteriocin lactococcin A (*87*). Although lactococcin A does not belong to class IIa, its immunity protein binds to the cell membrane (*88*) and contains an amphiphilic helix. That immunity protein, whose three-dimensional structure is not known, has been proposed to interact with the lactococcin A receptor in the membrane and thereby prevent the insertion of the corresponding bacteriocin into the cell surface (*87*). It seems likely that in the presence of the

appropriate receptor, the nascent α-helix of ImB2 in the C-terminal portion [known to be important for specificity of protection (*50*)] could become more defined, further expose the hydrophobic pocket, and assist recognition of the binding partner. It is tempting to speculate that this partner could be the intracellular portion of membrane-bound protein(s) in the mannose phosphotransferase system EII_t^{man}, the putative target for extracellular attack by class IIa bacteriocins (*42*−*45*).

CONCLUSIONS

Although there is a high degree of sequence conservation among class IIa bacteriocins, there is limited cross-reactivity between their associated immunity proteins and correspondingly weaker sequence homology. The first structure determined for a class IIa immunity protein, ImB2, shows that it is a compact, globular protein consisting of a four-helix bundle with a fifth α-helix and extended C-terminus that pack against helices 3 and 4. Helix 3 of ImB2 is well-defined from residue 44 to 55, and nascent helical structure is observed until residue 64. This region together with the hydrophobic pocket and the loop following, which contains a stretch of basic amino acids, may be important for binding interactions. To date, there are no other structures available for LAB bacteriocin immunity proteins. Sequence comparisons demonstrate that there is much variability in the amino acid composition of these proteins, although they are all quite hydrophobic in nature. Structure elucidations of other immunity proteins will reveal whether, as suspected, the four-helix bundle remains a conserved structural motif, and which regions of the proteins may be important for protein−protein interactions. The exact mechanism by which LAB immunity proteins afford protection to their cognate bacteriocins remains elusive. However, our results, combined with those showing that the specificity of immunity proteins was found to lie in the C-terminal half, suggest that interaction with another protein on the cytoplasmic side of the cell membrane, possibly a receptor in the mannose phosphotransferase system, may interfere with binding and/or lysis by class IIa bacteriocins. Interestingly, the immunity proteins for *E. coli* colicins with DNase or RNase activities also form four-helix bundles, suggesting an evolutionary conservation of structure, if not sequence or mechanism of action. Isolation of the membrane receptors for class IIa bacteriocins and investigation of their interactions on the molecular level with both bacteriocins and their associated immunity proteins will serve to further elucidate the manner in which the high degree of target specificity is achieved. Understanding of the three-dimensional structures of immunity proteins and their cognate class IIa bacteriocins provides a basis for this.

ACKNOWLEDGMENT

We thank Dr. Ryan T. McKay [National High Field Nuclear Magnetic Resonance Facility (NANUC), Edmonton, AB] and Dr. Albin Otter (Department of Chemistry, University of Alberta) for assistance with NMR experiments and Lara Silkin and Scott McGavin for technical assistance. All 800 MHz NMR spectra were recorded at the National High Field Nuclear Magnetic Resonance Facility (NANUC).

SUPPORTING INFORMATION AVAILABLE

Solution structures of class IIa bacteriocins (Figure S1), ^{15}N and ^{13}C chemical shifts for ImB2 (Table S1), and proton chemical shifts for ImB2 (Table S2). This material is available free of charge via the Internet at http://pubs.acs.org.

REFERENCES

1. Guder, A., Wiedemann, I., and Sahl, H. G. (2000) Posttranslationally modified bacteriocins: the lantibiotics, *Biopolymers 55*, 62−73.
2. Papagianni, M. (2003) Ribosomally synthesized peptides with antimicrobial properties: biosynthesis, structure, function, and applications, *Biotechnol. Adv. 21*, 465−499.
3. van Belkum, M. J., and Stiles, M. E. (2000) Nonlantibiotic antibacterial peptides from lactic acid bacteria, *Nat. Prod. Rep. 17*, 323−335.
4. Xie, L., Miller, L. M., Chatterjee, C., Averin, O., Kelleher, N. L., and van der Donk, W. A. (2004) Lacticin 481: in vitro reconstitution of lantibiotic synthetase activity, *Science 303*, 679−681.
5. Garneau, S., Martin, N. I., and Vederas, J. C. (2002) Two-peptide bacteriocins produced by lactic acid bacteria, *Biochimie 84*, 577−592.
6. van Kraaij, C., de Vos, W. M., Siezen, R. J., and Kuipers, O. P. (1999) Lantibiotics: biosynthesis, mode of action and applications, *Nat. Prod. Rep. 16*, 575−587.
7. Nes, I. F., and Holo, H. (2000) Class II antimicrobial peptides from lactic acid bacteria, *Biopolymers 55*, 50−61.
8. Ennahar, S., Sashihara, T., Sonomoto, K., and Ishizaki, A. (2000) Class IIa bacteriocins: biosynthesis, structure and activity, *FEMS Microbiol. Rev. 24*, 85−106.
9. Eijsink, V. G., Axelsson, L., Diep, D. B., Havarstein, L. S., Holo, H., and Nes, I. F. (2002) Production of class II bacteriocins by lactic acid bacteria; an example of biological warfare and communication, *Antonie Van Leeuwenhoek 81*, 639−654.
10. Hastings, J. W., Sailer, M., Johnson, K., Roy, K. L., Vederas, J. C., and Stiles, M. E. (1991) Characterization of leucocin A-UAL 187 and cloning of the bacteriocin gene from *Leuconostoc gelidum*, *J. Bacteriol. 173*, 7491−7500.
11. Quadri, L. E., Sailer, M., Roy, K. L., Vederas, J. C., and Stiles, M. E. (1994) Chemical and genetic characterization of bacteriocins produced by *Carnobacterium piscicola* LV17B, *J. Biol. Chem. 269*, 12204−12211.
12. Thompson, J. D., Higgins, D. G., and Gibson, T. J. (1994) CLUSTAL W: improving the sensitivity of progressive multiple sequence alignment through sequence weighting, position-specific gap penalties and weight matrix choice, *Nucleic Acids Res. 22*, 4673−4680.
13. Fimland, G., Eijsink, V. G., and Nissen-Meyer, J. (2002) Comparative studies of immunity proteins of pediocin-like bacteriocins, *Microbiology 148*, 3661−3670.
14. Marugg, J. D., Gonzalez, C. F., Kunka, B. S., Ledeboer, A. M., Pucci, M. J., Toonen, M. Y., Walker, S. A., Zoetmulder, L. C., and Vandenbergh, P. A. (1992) Cloning, expression, and nucleotide sequence of genes involved in production of pediocin PA-1, and bacteriocin from *Pediococcus acidilactici* PAC1.0, *Appl. Environ. Microbiol. 58*, 2360−2367.
15. Le Marrec, C., Hyronimus, B., Bressollier, P., Verneuil, B., and Urdaci, M. C. (2000) Biochemical and genetic characterization of coagulin, a new antilisterial bacteriocin in the pediocin family of bacteriocins, produced by *Bacillus coagulans* I(4), *Appl. Environ. Microbiol. 66*, 5213−5220.
16. Larsen, A. G., Vogensen, F. K., and Josephsen, J. (1993) Antimicrobial activity of lactic acid bacteria isolated from sour doughs: purification and characterization of bavaricin A, a bacteriocin produced by *Lactobacillus bavaricus* MI401, *J. Appl. Bacteriol. 75*, 113−122.
17. Tichaczek, P. S., Vogel, R. F., and Hammes, W. P. (1994) Cloning and sequencing of sakP encoding sakacin P, the bacteriocin produced by *Lactobacillus sake* LTH 673, *Microbiology 140*, 361−367.
18. Bennik, M. H. J., Vanloo, B., Brasseur, R., Gorris, L. G. M., and Smid, E. J. (1998) A novel bacteriocin with a YGNGV motif from vegetable-associated *Enterococcus mundtii*: full characterization and interaction with target organisms, *Biochim. Biophys. Acta 1373*, 47−58.
19. Kawamoto, S., Shima, J., Sato, R., Eguchi, T., Ohmomo, S., Shibato, J., Horikoshi, N., Takeshita, K., and Sameshima, T. (2002) Biochemical and genetic characterization of mundticin KS, an antilisterial peptide produced by *Enterococcus mundtii* NFRI 7393, *Appl. Environ. Microbiol. 68*, 3830−3840.

20. Jack, R. W., Wan, J., Gordon, J., Harmark, K., Davidson, B. E., Hillier, A. J., Wettenhall, R. E., Hickey, M. W., and Coventry, M. J. (1996) Characterization of the chemical and antimicrobial properties of piscicolin 126, a bacteriocin produced by *Carnobacterium piscicola* JG126, *Appl. Environ. Microbiol. 62*, 2897−2903.
21. Kalmokoff, M. L., Banerjee, S. K., Cyr, T., Hefford, M. A., and Gleeson, T. (2001) Identification of a new plasmid-encoded sec-dependent bacteriocin produced by *Listeria innocua* 743, *Appl. Environ. Microbiol. 67*, 4041−4047.
22. Fimland, G., Sletten, K., and Nissen-Meyer, J. (2002) The complete amino acid sequence of the pediocin-like antimicrobial peptide leucocin C, *Biochem. Biophys. Res. Commun. 295*, 826−827.
23. Kaiser, A. L., and Montville, T. J. (1996) Purification of the bacteriocin bavaricin MN and characterization of its mode of action against *Listeria monocytogenes* Scott A cells and lipid vesicles, *Appl. Environ. Microbiol. 62*, 4529−4535.
24. Metivier, A., Pilet, M. F., Dousset, X., Sorokine, O., Anglade, P., Zagorec, M., Piard, J. C., Marion, D., Cenatiempo, Y., and Fremaux, C. (1998) Divercin V41, a new bacteriocin with two disulphide bonds produced by *Carnobacterium divergens* V41: primary structure and genomic organization, *Microbiology 144*, 2837−2844.
25. Aymerich, T., Holo, H., Havarstein, L. S., Hugas, M., Garriga, M., and Nes, I. F. (1996) Biochemical and genetic characterization of enterocin A from *Enterococcus faecium*, a new antilisterial bacteriocin in the pediocin family of bacteriocins, *Appl. Environ. Microbiol. 62*, 1676−1682.
26. Simon, L., Fremaux, C., Cenatiempo, Y., and Berjeaud, J. M. (2002) Sakacin G, a new type of antilisterial bacteriocin, *Appl. Environ. Microbiol. 68*, 6416−6420.
27. van Reenen, C. A., Dicks, L. M., and Chikindas, M. L. (1998) Isolation, purification and partial characterization of plantaricin 423, a bacteriocin produced by *Lactobacillus plantarum*, *J. Appl. Microbiol. 84*, 1131−1137.
28. Fremaux, C., Hechard, Y., and Cenatiempo, Y. (1995) Mesentericin Y105 gene clusters in *Leuconostoc mesenteroides* Y105, *Microbiology 141*, 1637−1645.
29. Tichaczek, P. S., Vogel, R. F., and Hammes, W. P. (1993) Cloning and sequencing of curA encoding curvacin A, the bacteriocin produced by *Lactobacillus curvatus* LTH1174, *Arch. Microbiol. 160*, 279−283.
30. Cintas, L. M., Casaus, P., Havarstein, L. S., Hernandez, P. E., and Nes, I. F. (1997) Biochemical and genetic characterization of enterocin P, a novel sec-dependent bacteriocin from *Enterococcus faecium* P13 with a broad antimicrobial spectrum, *Appl. Environ. Microbiol. 63*, 4321−4330.
31. Ferchichi, M., Frere, J., Mabrouk, K., and Manai, M. (2001) Lactococcin MMFII, a novel class IIa bacteriocin produced by *Lactococcus lactis* MMFII, isolated from a Tunisian dairy product, *FEMS Microbiol. Lett. 205*, 49−55.
32. Eguchi, T., Kaminaka, K., Shima, J., Kawamoto, S., Mori, K., Choi, S. H., Doi, K., Ohmomo, S., and Ogata, S. (2001) Isolation and characterization of enterocin SE-K4 produced by thermophilic *enterococci*, *Enterococcus faecalis* K-4, *Biosci., Biotechnol., Biochem. 65*, 247−253.
33. Tomita, H., Fujimoto, S., Tanimoto, K., and Ike, Y. (1996) Cloning and genetic organization of the bacteriocin 31 determinant encoded on the *Enterococcus faecalis* pheromone-responsive conjugative plasmid pYI17, *J. Bacteriol. 178*, 3585−3593.
34. Fregeau-Gallagher, N. L., Sailer, M., Niemczura, W. P., Nakashima, T. T., Stiles, M. E., and Vederas, J. C. (1997) Three-dimensional structure of leucocin A in trifluoroethanol and dodecylphosphocholine micelles: spatial location of residues critical for biological activity in type IIa bacteriocins from lactic acid bacteria, *Biochemistry 36*, 15062−15072.
35. Wang, Y., Henz, M. E., Fregeau Gallagher, N. L., Chai, S., Gibbs, A. C., Yan, L. Z., Stiles, M. E., Wishart, D. S., and Vederas, J. C. (1999) Solution structure of carnobacteriocin B2 and implications for structure−activity relationships among type IIa bacteriocins from lactic acid bacteria, *Biochemistry 38*, 15438−15447.
36. Uteng, M., Hauge, H. H., Markwick, P. R., Fimland, G., Mantzilas, D., Nissen-Meyer, J., and Muhle-Goll, C. (2003) Three-dimensional structure in lipid micelles of the pediocin-like antimicrobial peptide sakacin P and a sakacin P variant that is structurally stabilized by an inserted C-terminal disulfide bridge, *Biochemistry 42*, 11417−11426.
37. Sprules, T., Kawulka, K. E., Gibbs, A. C., Wishart, D. S., and Vederas, J. C. (2004) NMR solution structure of the precursor for carnobacteriocin B2, an antimicrobial peptide from *Carnobacterium piscicola*, *Eur. J. Biochem. 271*, 1748−1756.
38. Kaur, K., Andrew, L. C., Wishart, D. S., and Vederas, J. C. (2004) Dynamic Relationships among Type IIa Bacteriocins: Temperature Effects on Antimicrobial Activity and on Structure of the C-Terminal Amphipathic α-Helix as a Receptor Binding Region, *Biochemistry 43*, 9009−9020.
39. Yan, L. Z., Gibbs, A. C., Stiles, M. E., Wishart, D. S., and Vederas, J. C. (2000) Analogues of bacteriocins: antimicrobial specificity and interactions of leucocin A with its enantiomer, carnobacteriocin B2, and truncated derivatives, *J. Med. Chem. 43*, 4579−4581.
40. Quadri, L. E., Yan, L. Z., Stiles, M. E., and Vederas, J. C. (1997) Effect of amino acid substitutions on the activity of carnobacteriocin B2. Overproduction of the antimicrobial peptide, its engineered variants, and its precursor in *Escherichia coli*, *J. Biol. Chem. 272*, 3384−3388.
41. Fimland, G., Eijsink, V. G., and Nissen-Meyer, J. (2002) Mutational analysis of the role of tryptophan residues in an antimicrobial peptide, *Biochemistry 41*, 9508−9515.
42. Dalet, K., Cenatiempo, Y., Cossart, P., and Hechard, Y. (2001) A sigma(54)-dependent PTS permease of the mannose family is responsible for sensitivity of *Listeria monocytogenes* to mesentericin Y105, *Microbiology 147*, 3263−3269.
43. Gravesen, A., Ramnath, M., Rechinger, K. B., Andersen, N., Jansch, L., Hechard, Y., Hastings, J. W., and Knochel, S. (2002) High-level resistance to class IIa bacteriocins is associated with one general mechanism in *Listeria monocytogenes*, *Microbiology 148*, 2361−2369.
44. Hechard, Y., Pelletier, C., Cenatiempo, Y., and Frere, J. (2001) Analysis of sigma(54)-dependent genes in *Enterococcus faecalis*: a mannose PTS permease (EII(Man)) is involved in sensitivity to a bacteriocin, mesentericin Y105, *Microbiology 147*, 1575−1580.
45. Ramnath, M., Beukes, M., Tamura, K., and Hastings, J. W. (2000) Absence of a putative mannose-specific phosphotransferase system enzyme IIAB component in a leucocin A-resistant strain of *Listeria monocytogenes*, as shown by two-dimensional sodium dodecyl sulfate-polyacrylamide gel electrophoresis, *Appl. Environ. Microbiol. 66*, 3098−3101.
46. O'Keeffe, T., Hill, C., and Ross, R. P. (1999) Characterization and heterologous expression of the genes encoding enterocin a production, immunity, and regulation in *Enterococcus faecium* DPC1146, *Appl. Environ. Microbiol. 65*, 1506−1515.
47. Axelsson, L., and Holck, A. (1995) The genes involved in production of and immunity to sakacin A, a bacteriocin from *Lactobacillus sake* Lb706, *J. Bacteriol. 177*, 2125−2137.
48. Dayem, M. A., Fleury, Y., Devilliers, G., Chaboisseau, E., Girard, R., Nicolas, P., and Delfour, A. (1996) The putative immunity protein of the Gram-positive bacteria *Leuconostoc mesenteroides* is preferentially located in the cytoplasm compartment, *FEMS Microbiol. Lett. 138*, 251−259.
49. Quadri, L. E., Sailer, M., Terebiznik, M. R., Roy, K. L., Vederas, J. C., and Stiles, M. E. (1995) Characterization of the protein conferring immunity to the antimicrobial peptide carnobacteriocin B2 and expression of carnobacteriocins B2 and BM1, *J. Bacteriol. 177*, 1144−1151.
50. Johnsen, L., Fimland, G., Mantzilas, D., and Nissen-Meyer, J. (2004) Structure−function analysis of immunity proteins of pediocin-like bacteriocins: C-terminal parts of immunity proteins are involved in specific recognition of cognate bacteriocins, *Appl. Environ. Microbiol. 70*, 2647−2652.
51. Zhang, O., Kay, L. E., Olivier, J. P., and Forman-Kay, J. D. (1994) Backbone ^{1}H and ^{15}N resonance assignments of the N-terminal SH3 domain of drk in folded and unfolded states using enhanced-sensitivity pulsed field gradient NMR techniques, *J. Biomol. NMR 4*, 845−858.
52. Kay, L. E., Keifer, P., and Saarinen, T. (1992) Pure Absorption Gradient Enhanced Heteronuclear Single Quantum Correlation Spectroscopy with Improved Sensitivity, *J. Am. Chem. Soc. 114*, 10663−10665.
53. Vuister, G. W., and Bax, A. (1993) Quantitative J Correlation: A New Approach for Measuring Homonuclear 3-Bond $J_{HNH\alpha}$ Coupling-Constants in N-15-Enriched Proteins, *J. Am. Chem. Soc. 115*, 7772−7777.
54. Kuboniwa, H., Grzesiek, S., Delaglio, F., and Bax, A. (1994) Measurement of H-N-H-α J-Couplings in Calcium-Free Calmodulin Using New 2D and 3D Water-Flip-Back Methods, *J. Biomol. NMR 4*, 871−878.

55. Grzesiek, S., and Bax, A. (1992) Improved 3D Triple-Resonance NMR Techniques Applied to a 31-KDa Protein, *J. Magn. Reson. 96*, 432−440.
56. Ikura, M., Kay, L. E., and Bax, A. (1990) A Novel-Approach for Sequential Assignment of H-1, C-13, and N-15 Spectra of Larger Proteins: Heteronuclear Triple-Resonance 3-Dimensional NMR Spectroscopy: Application to Calmodulin, *Biochemistry 29*, 4659−4667.
57. Kay, L. E., Xu, G. Y., and Yamazaki, T. (1994) Enhanced-Sensitivity Triple-Resonance Spectroscopy with Minimal H_2O Saturation, *J. Magn. Reson., Ser. A 109*, 129−133.
58. Muhandiram, D. R., and Kay, L. E. (1994) Gradient-Enhanced Triple-Resonance 3-Dimensional NMR Experiments with Improved Sensitivity, *J. Magn. Reson., Ser. B 103*, 203−216.
59. Wittekind, M., and Mueller, L. (1993) HNCACB, a High-Sensitivity 3D NMR Experiment to Correlate Amide-Proton and Nitrogen Resonances with the α-Carbon and β-Carbon Resonances in Proteins, *J. Magn. Reson., Ser. B 101*, 201−205.
60. Grzesiek, S., and Bax, A. (1992) Correlating Backbone Amide and Side-Chain Resonances in Larger Proteins by Multiple Relayed Triple Resonance NMR, *J. Am. Chem. Soc. 114*, 6291−6293.
61. Sattler, M., Schwendinger, M. G., Schleucher, J., and Griesinger, C. (1995) Novel Strategies for Sensitivity Enhancement in Heteronuclear Multidimensional NMR Experiments Employing Pulsed-Field Gradients, *J. Biomol. NMR 6*, 11−22.
62. Pascal, S. M., Muhandiram, D. R., Yamazaki, T., Forman-Kay, J. D., and Kay, L. E. (1994) Simultaneous Acquisition of N-15-Edited and C-13-Edited NOE Spectra of Proteins Dissolved in H_2O, *J. Magn. Reson., Ser. B 103*, 197−201.
63. Wishart, D. S., Bigam, C. G., Yao, J., Abildgaard, F., Dyson, H. J., Oldfield, E., Markley, J. L., and Sykes, B. D. (1995) ^1H, ^{13}C and ^{15}N chemical shift referencing in biomolecular NMR, *J. Biomol. NMR 6*, 135−140.
64. Delaglio, F., Grzesiek, S., Vuister, G. W., Zhu, G., Pfeifer, J., and Bax, A. (1995) NMRPipe: a multidimensional spectral processing system based on UNIX pipes, *J. Biomol. NMR 6*, 277−293.
65. Johnson, B. A., and Blevins, R. A. (1994) NMR View: a Computer-Program for the Visualization and Analysis of NMR Data, *J. Biomol. NMR 4*, 603−614.
66. Gagne, S. M., Tsuda, S., Li, M. X., Chandra, M., Smillie, L. B., and Sykes, B. D. (1994) Quantification of the Calcium-Induced Secondary Structural-Changes in the Regulatory Domain of Troponin-C, *Protein Sci. 3*, 1961−1974.
67. Baxter, N. J., and Williamson, M. P. (1997) Temperature dependence of ^1H chemical shifts in proteins, *J. Biomol. NMR 9*, 359−369.
68. Brunger, A. T., Adams, P. D., Clore, G. M., DeLano, W. L., Gros, P., Grosse-Kunstleve, R. W., Jiang, J. S., Kuszewski, J., Nilges, M., Pannu, N. S., Read, R. J., Rice, L. M., Simonson, T., and Warren, G. L. (1998) Crystallography & NMR system: A new software suite for macromolecular structure determination, *Acta Crystallogr. D54*, 905−921.
69. Wishart, D. S., and Sykes, B. D. (1994) The ^{13}C chemical-shift index: a simple method for the identification of protein secondary structure using ^{13}C chemical-shift data, *J. Biomol. NMR 4*, 171−180.
70. Chothia, C., Levitt, M., and Richardson, D. (1981) Helix to helix packing in proteins, *J. Mol. Biol. 145*, 215−250.
71. Kamtekar, S., and Hecht, M. H. (1995) The four-helix bundle: what determines a fold? *FASEB J. 9*, 1013−1022.
72. Carr, S., Walker, D., James, R., Kleanthous, C., and Hemmings, A. M. (2000) Inhibition of a ribosome-inactivating ribonuclease: the crystal structure of the cytotoxic domain of colicin E3 in complex with its immunity protein, *Struct. Folding Des. 8*, 949−960.
73. Soelaiman, S., Jakes, K., Wu, N., Li, C., and Shoham, M. (2001) Crystal structure of colicin E3: implications for cell entry and ribosome inactivation, *Mol. Cell 8*, 1053−1062.
74. Dennis, C. A., Videler, H., Pauptit, R. A., Wallis, R., James, R., Moore, G. R., and Kleanthous, C. (1998) A structural comparison of the colicin immunity proteins Im7 and Im9 gives new insights into the molecular determinants of immunity-protein specificity, *Biochem. J. 333*, 183−191.
75. Chak, K. F., Safo, M. K., Ku, W. Y., Hsieh, S. Y., and Yuan, H. S. (1996) The crystal structure of the immunity protein of colicin E7 suggests a possible colicin-interacting surface, *Proc. Natl. Acad. Sci. U.S.A. 93*, 6437−6442.
76. Hsieh, S. Y., Ko, T. P., Tseng, M. Y., Ku, W., Chak, K. F., and Yuan, H. S. (1997) A novel role of ImmE7 in the autoregulatory expression of the ColE7 operon and identification of possible RNase active sites in the crystal structure of dimeric ImmE7, *EMBO J. 16*, 1444−1454.
77. Boetzel, R., Czisch, M., Kaptein, R., Hemmings, A. M., James, R., Kleanthous, C., and Moore, G. R. (2000) NMR investigation of the interaction of the inhibitor protein Im9 with its partner DNase, *Protein Sci. 9*, 1709−1718.
78. Kuhlmann, U. C., Pommer, A. J., Moore, G. R., James, R., and Kleanthous, C. (2000) Specificity in protein−protein interactions: the structural basis for dual recognition in endonuclease colicin-immunity protein complexes, *J. Mol. Biol. 301*, 1163−1178.
79. Osborne, M. J., Breeze, A. L., Lian, L.-Y., Reilly, A., James, R., Kleanthous, C., and Moore, G. R. (1996) Three-dimensional solution structure and ^{13}C magnetic resonance assignments of the Colicin E9 protein Im9, *Biochemistry 35*, 9505−9512.
80. Kolade, O. O., Carr, S. B., Kuhlmann, U. C., Pommer, A., Kleanthous, C., Bouchcinsky, C. A., and Hemmings, A. M. (2002) Structural aspects of the inhibition of DNase and rRNase colicins by their immunity proteins, *Biochimie 84*, 439−446.
81. Ko, T. P., Liao, C. C., Ku, W. Y., Chak, K. F., and Yuan, H. S. (1999) The crystal structure of the DNase domain of colicin E7 in complex with its inhibitor Im7 protein, *Struct. Folding Des. 7*, 91−102.
82. Espesset, D., Duche, D., Baty, D., and Geli, V. (1996) The channel domain of colicin A is inhibited by its immunity protein through direct interaction in the *Escherichia coli* inner membrane, *EMBO J. 15*, 2356−2364.
83. Pilsl, H., and Braun, V. (1995) Evidence that the immunity protein inactivates colicin 5 immediately prior to the formation of the transmembrane channel, *J. Bacteriol. 177*, 6966−6972.
84. Eijsink, V. G., Skeie, M., Middelhoven, P. H., Brurberg, M. B., and Nes, I. F. (1998) Comparative studies of class IIa bacteriocins of lactic acid bacteria, *Appl. Environ. Microbiol. 64*, 3275−3281.
85. Koradi, R., Billeter, M., and Wuthrich, K. (1996) MOLMOL: a program for display and analysis of macromolecular structures, *J. Mol. Graphics 14*, 51−55.
86. Kraulis, P. J. (1991) Molscript: A Program to Produce Both Detailed and Schematic Plots of Protein Structures, *J. Appl. Crystallogr. 24*, 946−950.
87. Venema, K., Haverkort, R. E., Abee, T., Haandrikman, A. J., Leenhouts, K. J., de Leij, L., Venema, G., and Kok, J. (1994) Mode of action of LciA, the lactococcin A immunity protein, *Mol. Microbiol. 14*, 521−532.
88. Nissen-Meyer, J., Havarstein, L. S., Holo, H., Sletten, K., and Nes, I. F. (1993) Association of the lactococcin A immunity factor with the cell membrane: purification and characterization of the immunity factor, *J. Gen. Microbiol. 139*, 1503−1509.
89. Koradi, R., Billeter, M., and Wuthrich, K. (1996) MOLMOL: a program for display and analysis of macromolecular structures, *J. Mol. Graphics 14*, 29−32.

BI048854+